

Relationship between atmospheric blocking and warm season thunderstorms over western and central Europe

Susanna Mohr^{a,b*}, Jan Wandel^a, Sina Lenggenhager^c, Olivia Martius^{c,d}

^a *Institute of Meteorology and Climate Research (IMK-TRO), Karlsruhe Institute of Technology (KIT), Karlsruhe, Germany*

^b *Center for Disaster Management and Risk Reduction Technology, KIT, Germany*

^c *Oeschger Centre for Climate Change Research and Institute of Geography, University of Bern, Bern, Switzerland*

^d *Mobilier Lab for Natural Risks, University of Bern, Bern, Switzerland*

*Correspondence to: S. Mohr, Institute of Meteorology and Climate Research (IMK-TRO), KIT, Hermann-von-Helmholtz-Platz 1, 76344 Eggenstein-Leopoldshafen, Karlsruhe, Germany. E-mail:mohr@kit.edu

This article has been accepted for publication and undergone full peer review but has not been through the copyediting, typesetting, pagination and proofreading process, which may lead to differences between this version and the Version of Record. Please cite this article as doi: 10.1002/qj.3603

A statistically significant link is presented between atmospheric blocking located over the eastern North Atlantic and northern Europe and warm season thunderstorm activity over western and central Europe. Lightning data from 2001 to 2014 were used to identify thunderstorm days and blocking events were extracted from the ERA-Interim reanalysis using an objective identification algorithm. The statistical link between the two phenomena is established by the odds ratio analysis. Two areas one over the eastern part of the North Atlantic and one over the Baltic Sea were identified, where blocking influences the occurrence of deep moist convection in parts of western and central Europe.

Based on the mean ambient conditions on days with blocking in these two areas, well-known dynamic and thermodynamic mechanisms supporting or suppressing the development of thunderstorms were confirmed. The anticyclonic circulation of a block over the eastern part of the North Atlantic leads to a northerly to northwesterly advection of dry and stable air masses into Europe on the eastern flank of the block. In addition, these environmental conditions are on average associated with large-scale subsidence of air masses (convection-inhibiting conditions). In contrast, the southerly to southwesterly advection of warm, moist and unstable air masses on the western flank of a block over the Baltic Sea results in convection-favouring conditions over western and central Europe. Both blocking situations are on average associated with weak wind speeds at mid-tropospheric levels and with weak wind shear. As a consequence, thunderstorms related to atmospheric blocking over the Baltic Sea tend to be on average less organised.

Key Words: Atmospheric blocking; thunderstorms; deep moist convection; Europe; odds ratio; ambient conditions; wind shear

Received ...

Introduction

During the last decades, various studies have established a link between atmospheric blocking and different weather situations (e.g., Sillmann and Croci-Maspoli 2009; Brunner *et al.* 2018; Sousa *et al.* 2018; Woollings *et al.* 2018). Atmospheric blocks with a lifetime of several days to weeks are quasi-stationary persistent flow patterns that modify mid-latitude storm tracks (Rex 1950a,b; Barriopedro *et al.* 2006; Woollings *et al.* 2018). Consequently, blocks influence the intensity and frequency of weather extremes like cold spells and heat waves in regions upstream or downstream of the blocked area. For example during the European winter, blocking over the North Atlantic supports a northeasterly inflow of cold and

dry air masses from high- to mid-latitudes (Sillmann *et al.* 2011). In summer, the increase of shortwave radiation during the day due to clear sky conditions and adiabatic warming (due to large-scale descent) are important driving factors of surface heating (Bieli *et al.* 2015). In addition, warm air advection to the western sector of the block can contribute to warm anomalies within blocks (e.g., the Russian heat wave 2010; Trenberth and Fasullo 2012; Quandt *et al.* 2017). A relation also exists between blocking and heavy precipitation or flood events (including flash floods; e.g., Sousa *et al.* 2017; Lenggenhager *et al.* 2018; Lenggenhager and Martius 2019). For example, the central European flood in June 2013 (Schröter *et al.* 2015) was influenced by an Atlantic blocking regime that resulted in cool and unusually wet conditions due to repeated Rossby wave-breaking over Europe (Grams *et al.* 2014). In the case of the 2010 Pakistan flooding, the record-breaking event resulted from the interaction between a blocking ridge with associated Rossby wave-breaking, monsoon surges, extratropical disturbances, and topography (Hong *et al.* 2011; Martius *et al.* 2013).

First case studies suggest a relation between blocking and warm season thunderstorms. For example, Piper *et al.* (2016) show that an exceptional sequence of severe thunderstorms causing several flash floods in May and June 2016 in Germany was fostered by high atmospheric moisture content, enhanced thermodynamic instability, weak wind speed, and large-scale lifting by surface lows. These convection-favouring conditions persisted over almost two weeks and were associated first with Scandinavian blocking and later with European blocking (cf. Grams *et al.* 2017). In May 2018 a blocking anticyclone over northern Europe, associated with repeated cut-off lows forming along its southern flank, led to heavy precipitation and flash floods in western and central Europe (Mohr *et al.* 2019). In this case, the flow pattern provided key ingredients of stationary convection: moist air mass being trapped in the block and local-scale ascent via a cut-off low. A recent study by Santos and Belo-Pereira (2019) also found a relationship between blocking and hail events in Portugal.

The synoptic situation creates the environment for the development of thunderstorm (e.g., Doswell *et al.* 1996). For example, Wapler and James (2015) identified various circulation types relevant for the occurrence of thunderstorms in central Europe on the basis of an objective method for classifying synoptic patterns. In all these pattern, thunderstorms move in a direction from southwest to northeast; thunderstorms moving from the northwestern, northern or eastern directions are far less common. Piper (2017) and Piper *et al.* (2019) also found that the most prominent circulation pattern in terms of thunderstorm activity

is a southwesterly mid-tropospheric flow type. The southwesterly flow direction in connection with the occurrence of thunderstorms (and hail) in western and central Europe has also been observed by other studies (Bertram and Mayr 2004; Kunz *et al.* 2009; Kapsch *et al.* 2012; Mohr 2013; Merino *et al.* 2014; Nisi *et al.* 2016), because this pattern supports the advection of convection-favouring air masses (subtropical, often conditionally unstable) to Europe by low-pressure systems ahead of the upper-tropospheric trough.

Atmospheric blocks may influence the occurrence and persistence of such thunderstorm favouring flow patterns.

The goal of this study is to establish a statistical link between blocking and thunderstorm days. The first aim of the study is to identify areas where the occurrence of blocking influences the thunderstorm activity over western and central Europe. The second aim is to characterise the relevant atmospheric mechanisms and processes (e.g., air masses, flow regimes) that link convective storms and atmospheric blocks. We investigate only thunderstorm activity in general and do not distinguish the severity of thunderstorms (e.g., thunderstorms associated with phenomena such as hail or heavy rain events).

The paper is structured as follows: Section 2 provides a short overview of data sets and statistical methods used in this study. Section 3 describes the methodological procedure identifying relevant areas, in which blocking is frequently observed and which are related to thunderstorms in Europe. In Section 4, we establish the statistical relation between blocking and thunderstorm activity in different parts of Europe. Subsequently, we assess the relevant environmental conditions during days with blocking by individual case studies and anomaly composites (Sect. 5). Finally, Section 6 summarises the results and draws conclusions.

2. Data sets and methods

In Europe, thunderstorms occur predominantly during the summer half year (Finke and Hauf 1996; Wapler 2013; Anderson and Klugmann 2014; Poelman *et al.* 2016; Piper and Kunz 2017; Taszarek *et al.* 2019). Because the study area covers western and central Europe, our analyses concentrate on the four warmest months with the highest thunderstorm activity (May – August; Anderson and Klugmann 2014; Poelman *et al.* 2016; Piper and Kunz 2017; Taszarek *et al.* 2019).

2.1. Lightning data

The correlation between thunderstorm activity and atmospheric blocking is examined using data from the ground-based low-frequency lightning detection system BLIDS (BLitz-Informationen-Dienst Siemens),

which is part of the EUCLID (EUropean Cooperation for LIghtning Detection) network (Drüe *et al.* 2007; Schulz *et al.* 2016; Poelman *et al.* 2016). The lightning data were available for a 14-year period (2001 – 2014) and contain a large area in western and central Europe covering France, Benelux (Belgium, Netherlands, Luxembourg), Germany, Switzerland and Austria. We use an objective definition of the dichotomous variable *thunderstorm day* (TD). A TD is defined if at least five cloud-to-ground flashes were registered within a detection area of $10 \times 10 \text{ km}^2$ between 00:00 to 00:00 local time on the next day. This threshold was determined by an objective method by Piper and Kunz (2017) for the same detection area. The binary measure (TD yes/no) is—in contrast to lightning density—not dominated by single severe thunderstorms with several tens of thousands of flashes. More details about lightning data and the thunderstorm day classification method can be found in Piper and Kunz (2017).

Figure 1 shows the mean annual number of thunderstorm days from May to August, which is in good agreement with previous analyses of the spatial distribution of thunderstorm days in European countries (Wapler 2013; Anderson and Klugmann 2014; Poelman *et al.* 2016; Piper and Kunz 2017; Taszarek *et al.* 2019). Small differences to other TD probability maps result mainly from varying threshold definitions for a TD, from consideration of other time periods (especially the considered months), and/or the spatial resolution (detection area) of the TD map.

2.2. ERA-Interim reanalysis data

We use the European Centre for Medium-Range Weather Forecasts (ECMWF) ERA-Interim reanalysis (Dee *et al.* 2011) to identify atmospheric blocking (see Sect. 2.3) and to derive environmental conditions (e.g., stability measures, deep layer shear) during blocking situations. The blocking data are calculated on a $1.5^\circ \times 1^\circ$ longitude-latitude grid every 6 hours, whereas parameters describing the environmental conditions were available on a $0.75^\circ \times 0.75^\circ$ grid. The period for the statistical analysis (see Sect. 2.4) covers 2001 to 2014, for which lightning observations are available. For the climatological analysis including anomaly investigations, we use the period from 1981 to 2010 in the study.

2.3. Blocking data

In our study atmospheric blocks are defined as persistent negative upper-level potential vorticity (PV) anomalies based on the methodology of Schwierz *et al.* (2004): In the first step, vertically averaged PV values (between 500 and 150 hPa) are retrieved from the ERA-Interim. Then, the anomalies are calculated

at each grid point with respect to the multi-year (1979–2015) 30-day running mean centered at each time step. After applying a 2-day running mean to these vertically averaged PV anomalies, regions with less than -1 pvu are defined as blocks if they meet the two criteria: i) a persistence of at least five consecutive days and ii) a spatial overlap of at least 70 % of the area between two consecutive time steps. In contrast to Schwierz *et al.* (2004), a less strict PV anomaly threshold is chosen to avoid an underestimation of summer blocking (Crocini-Maspoli *et al.* 2007; Villiger 2017). A similar method was chosen by Pfahl and Wernli (2012), who used an even higher threshold of -0.7 pvu. Figure 2 shows the relative blocking frequency for the study period, where the maximum is located over the Atlantic basin (cf. Lenggenhager and Martius 2019).

2.4. Statistical methods

Both blocking and thunderstorm day data are available as binary time series (yes/no) for every summer day of the 14-year period. From these data, we calculate the odds ratio (OR; Backhaus *et al.* 2016), which quantifies the statistical relation or non-independence between two binary time series. Mathematically, the odds are calculated as the quotient of the probability (p) that an event will occur and the probability that it will not occur ($1 - p$). The OR can hence be computed from two probabilities $p(A)$ (blocking supports thunderstorm activity, $p_{\text{Block}}(\text{TD})$) and $p(B)$ (blocking suppresses thunderstorm activity, $p_{\text{Block}}(\overline{\text{TD}})$):

$$OR = \frac{\text{odds}(A)}{\text{odds}(B)} = \frac{\frac{p(A)}{1-p(A)}}{\frac{p(B)}{1-p(B)}} = \frac{p(A) \cdot (1 - p(B))}{p(B) \cdot (1 - p(A))} . \quad (1)$$

Logistic regression is one way of calculating the OR. In order to take into account the dependence between successive events, we used an autoregressive logistic regression model of the following form (following the procedure of Mahlstein *et al.* 2012):

$$\text{logit}(p(t)) = \beta_0 + \beta_1 y(t - 1) + \beta_2 y(t - 2) + \beta_3 \text{Block}(t) , \quad (2)$$

where $y(\cdot)$ is a binary time series indicating whether or not a TD occurred at the considered grid point; $\text{Block}(t)$ is also a binary time series indicating if there was blocking at time t . Mahlstein *et al.* (2012, see also auxiliary material) found that an increase in the autoregressive part to a higher order than 2 does not improve the model. Thus, the OR corresponds in the case of Equation (2) to $\exp(\beta_3)$, which can be seen as a multiplicative factor:

OR>1: The odds of the first group A is larger. This means for example if there is blocking, the odds of a TD increase.

OR<1: The odds of the first group A is smaller. This means for example if there is blocking, the odds for a TD decrease or if there is no blocking, the odds of a TD increase.

OR=1: No difference between both groups.

To assess the statistical significance of the anomalous environmental conditions associated with blocking (Sect. 5.2), we conduct a bootstrap test with replacement of the investigated meteorological values on each grid point in the investigated area (following the methodology of Scherrer *et al.* 2006). Thus, depending on the number of blocks n that are observed between 2001 and 2014 (cf. Table 1), 1,000 new samples with length n are created randomly with replacement from all event days in the 14-year period. Based on the 1,000 samples, we get a distribution function (here of the mean value), which we then compare to the observed anomaly during blocking. The null hypothesis is rejected for a specific grid point if the anomalous environmental condition in the blocking case is smaller than the 2.5 % or greater than the 97.5 % quantile of the distribution.

3. Methodological approach

The first aim is to identify regions over the North Atlantic and European sector, where blocking is related to thunderstorm activity (TDs) over Europe. For this purpose, all binary TD time series with a horizontal resolution of $10 \times 10 \text{ km}^2$ from 2001 to 2014 (May to August) are converted to the coarser resolution of the blocking data of $1^\circ \times 1^\circ$ (= one grid point, GP) resulting in 197 GPs. Subsequently, only GPs, where convective activity is frequently observed between May and August, are considered. We chose a threshold of at least five TDs per year per GP resulting in 132 GPs. This procedure excludes areas that tend to an overinterpretation of OR values due to low thunderstorm activity.

In a second step, the OR (see Sect. 2.4) is computed for each of these 132 GPs between binary TD time series and all grid points with binary blocking data (between 30°N and 70°N and 40°W and 40°E ; cf. examples in Fig. 3) by using an autoregressive logistic regression model (see Eq. 2). The continuous investigated area of the 132 GPs is in the following referred to as FOCREG (focus region; black line in Fig. 1). This procedure allows us to identify areas where the occurrence of blocking significantly increases

or decreases the odds of a TD in the FOCREG. Figure 3 shows examples of two cases (only OR with p-value of at least 95 % significance level are shown): (a) 48°N 4°E in northeastern France and (b) 52°N 11°E in central Germany (reference area in orange in Fig. 3). Both figures show an area over the eastern North Atlantic (blue colours), where the blocking occurrence leads to a reduction of the odds of TDs. In addition, an area over Northern Europe (mainly Baltic Sea) is indicated, where blocking occurrence increases the odds of TDs. For example, blocking over the Baltic Sea increases the odds of a TD in central Germany by a factor of at least three (Fig. 3a).

In the next step, the results of all 132 GPs (such as Fig. 3) are aggregated for each GP and we quantify how often $OR > 1$ (blocking supports TDs; red in Fig. 3) or $OR < 1$ (blocking suppresses TDs; blue in Fig. 3). This results in two areas (Fig. 4), where the occurrence of blocking has an important influence—whether supportive or suppressive—on the thunderstorm occurrence in western and central Europe. The first one, where the occurrence of blocking decreases TD probability, is found over the eastern North Atlantic (Celtic Sea, Ireland Wales, England and northwest France). The second area, where blocking increases the TD probability, is located over Northern Europe—mainly over southern Sweden, the Baltic Sea and adjacent region and the northern parts of Poland. This relation is observed in up to 70 to 80 % of the 132 cases for some grid points (see Fig. 4).

To objectively delimit the two areas, we use only GPs, where at least 40 % ($threshold_1$) of the cases (53 of 132 GPs from FOCREG; Fig. 4 black lines), show a (significant) relation between blocking and TDs. This results in 125 GPs for the area over the eastern North Atlantic (NA) with 62 GPs (1 = West) and 63 GPs (2 = East) and 130 GPs for the area over the Baltic Sea (BS) with 68 GPs (3 = West) and 62 GPs (4 = East; Fig. 4). The two areas are divided for further investigations. Referring back to the mean annual blocking frequency (see Fig. 2) shows that on average a block occurs in 10 to 20 % of the days in these two regions.

4. Relationship between blocking and European thunderstorm activity

In the next step, we calculate the OR between each of the areas (NA, NA West, NA East, BS, BS West, BS East) and the TD time series (now at the original resolution of the $10 \times 10 \text{ km}^2$; cf. Fig. 1). This provides findings about the influence of blocking in each of these six regions on thunderstorm activity in western and central Europe. For this, time series for each identified area are created, where a day is indicated as a blocking day (block = yes) if a block covers at least 20 % ($threshold_2$) of the defined area in Figure 5. Both

thresholds (threshold_1 , threshold_2) above are tested by sensitivity studies, which show very similar results or signals regarding relevant areas and OR values.

This procedure leads on average to 23–27 blocking days per summer season (19–22%). The annual number of blocking days varies between 11 and 47 (Table 1 left). Blocking over the North Atlantic is most frequent in May and June, while blocking over the Baltic Sea occurs almost twice as often in July compared to May and August (Table 1 right). The latter is in accordance with Lenggenhager and Martius (2019), who also found a high summer blocking frequency in a similar region. Note that July is also the month with the highest thunderstorm activity in central Europe (e.g., Anderson and Klugmann 2014; Piper and Kunz 2017). Both blocking and thunderstorm activity (Mohr *et al.* 2015a; Piper and Kunz 2017; Madonna *et al.* 2018; Merino *et al.* 2019) show a high year-to-year variability.

The presence of a block in all areas (NA/BS) is significantly linked to the thunderstorm activity in almost the entire investigation area (Figure 5). Note that only GPs (lightning grid: $10 \times 10 \text{ km}^2$) with an average of at least three TDs per year (cf. Fig. 1) are taken into account for calculating OR values. Here, we applied a lower TD threshold of three TDs due to the higher spatial resolution of $10 \times 10 \text{ km}^2$ to exclude similar areas with low thunderstorm activity as with the analyses on the $1^\circ \times 1^\circ$ grid (five TDs). While blocking in the NA area (Fig. 5 left) is primarily related to a reduction of TD frequency in central and northeastern France, Benelux, Switzerland, and the western part of Germany (exceptions exist near the Maritime Alps in France and the Cantabrian Mountains in Spain; red in Fig. 5 left), blocking in the BS area is associated with increased TD frequency throughout the investigation area (Fig. 5 right). For blocking over the NA, most of the OR values are between 0.27 and 0.46 (25 to 75 % quantile of values in Fig. 5a-c) indicating a strong reduction of the odds. The effect is strongest over central and northeastern France and along the North Sea coastline. Here, we find values below 0.28. For blocking in the BS area, the OR values are between 1.83 and 2.47 (25 to 75 % quantile of values in Fig. 5d-f), which corresponds approximately to a doubling of the odds of TDs. The relation is strongest over eastern Germany (especially for BS East) and lowest over the middle of Southern France (Massif Central; especially for BS East), southern Germany and Austria (especially for BS and BS West).

A slight shift of the areas, where a relationship exists, from west to east is evident with the division of the areas into west and east. Thus, in the case of both blocking in the NA area (Fig. 5b,c) and BS area (Fig. 5e,f), the high OR value (strong correlation) shifts from France to Germany—in particular to eastern

Germany. In Figure 5f, OR values of up to 6 are reached in eastern Germany, which corresponds to a six-fold increase of the odds of a TD. A significant correlation can also be seen in the eastern part of Austria. In contrast, blocking in the NA East area results in a substantial reduction of the probability for a TD over the German coast to the Baltic Sea (Fig. 5c). Note that the splitting of the two areas into a western and an eastern part in general does not change the sign of the odds signal (only for values close to zero). The tendency at each grid point is the same for Figure 5b–c and 5d–f. The splitting only influence the values (strength) and the statistical significance at each grid point. Furthermore, note that studies of OR analyses (NA/BS) carried out separately for each of the four months show similar results (robust signal; not shown). Due to a substantially reduced sample size, the results are, however, less significant.

In addition, it should be pointed out that there are also cases with blocking located over both areas (NA and BS) at the same time (so-called crossover cases). This means that the blocked area is large enough to cover both Great Britain and the Baltic Sea. This applies to 6 % of all days in the 14-year period or about a quarter of all blocks. A calculation of the OR for the crossover cases shows—due to the small sample size—only statistical significance in a small region on the Mediterranean coast in south-eastern France (Provence-Alpes-Côte d’Azur) and over the Pyrenees, a mountain range between Spain and France, with an increased probability of thunderstorm development (equivalent to BS events; see Fig. 6b). The pure OR values (even those that are not significant; see Fig. 6a) indicate a tendency particularly over Benelux and Northern France (Hauts-de-France) to suppress thunderstorms (equivalent to NA events).

Environmental conditions during blocking

Because the OR only provides knowledge on the co-occurrence between blocking and thunderstorm activity and not on the causality of related atmospheric processes, the following section explores prevailing environmental conditions during days with blocking in both areas (NA, BS). The aim is to identify large-scale mechanisms that support or suppress local-scale thunderstorm activity. The hypothesis is that similar conditions like certain flow situations, associated moisture transports, or synoptic lifting mechanisms prevail during blocking episodes, which are convection-favouring or convection-inhibiting. The following meteorological parameters are investigated:

- (a) mid- and upper-troposphere flow and deep layer shear (Φ_{500} , PV, DLS),
- (b) atmospheric stability (SLI, CAPE, LR).

(c) moisture content (PW) and

(d) vertical winds (OMEGA).

The used acronyms stand for the geopotential in 500 hPa (Φ_{500}), PV on the isentrope of $\theta = 335$ K (useful during summertime, cf. R othlisberger *et al.* 2018), deep layer wind shear between 950 hPa and 500 hPa (DLS), surface-based Lifted Index (SLI), convective available potential energy (CAPE), lapse rate between 700 hPa and 500 Pa (LR), precipitable water (PW) and vertical motion at 500 hPa (OMEGA). On the one hand, we examine parameters that capture large-scale conditions (Φ_{500} , PV, OMEGA) and, on the other hand, parameters that have already shown a significant relationship to (severe) thunderstorms and their associated perils in numerous studies (SLI, CAPE, LR, DLS, PW e.g. Haklander and van Delden 2003; Manzato 2003; Kaltenb ock *et al.* 2009; S anchez *et al.* 2009; Mohr 2013; Westermayer *et al.* 2016; Taszarek *et al.* 2017).

In the following, only Φ_{500} , DLS, SLI, PW and OMEGA are considered and discussed in detail for two case studies (one NA & one BS case) and for all blocking events over NA and BS using anomaly composites. All variables are composited at 12 UTC, which is frequently used for investigating prevailing ambient conditions of severe thunderstorms in central Europe (Haklander and van Delden 2003; Kapsch *et al.* 2012; Mohr and Kunz 2013; Mohr *et al.* 2015b; Piper *et al.* 2019), which typically peak during late afternoon (Wapler 2013; Poelman *et al.* 2016; Piper and Kunz 2017).

5.1 Case studies

First, we examine several meteorological parameters using the example of blocking in the BS area on 10 July 2002 and in the NA area on 19 June 2001 (Fig. 7 and 8). On 10 July 2002 the upper- and mid-tropospheric circulation was dominated by a broad trough located over the northwestern part of the continent, which was associated with low-level southwesterly to southerly flow bringing warm and moist air masses from the Iberian Peninsula towards central Europe. Already early in the morning, first thunderstorms formed over northeast France (Fig. 7b). During the morning, the thunderstorms moved northeastward and reached the southwestern part of Germany. Additional deep moist convection formed during the day—first over the western part of Central Germany (Saarland and the Rhineland Palatinate), later also in southern Germany (Baden-Wuerttemberg and Bavaria). In the afternoon, scattered thunderstorms merged into a squall line that moved further northeast during the afternoon. The squall

line was a *derecho* associated with very high lightning frequency especially in eastern Germany (Fig. 7b) and which caused major damage by heavy rainfall, hail and in particular wind gusts up to hurricane force (Gatzen 2004). A maximum gust of 42 m s^{-1} was observed in Germany's capital, Berlin, where four people died and numerous others were injured (more details see Gatzen 2004).

On that day, blocking was present over Scandinavian and the Baltic Sea region (BS case; Fig. 7a grey contour), which went concurrently with a southwesterly to southerly mid-tropospheric flow over the investigation area. This flow direction is a typical situation in central Europe, which supports the development of thunderstorms, as this pattern favours the advection of convection-favouring air masses to central Europe (Kapsch *et al.* 2012; Merino *et al.* 2014; Wapler and James 2015; Nisi *et al.* 2016; Trefalt *et al.* 2018; Piper *et al.* 2019). Air masses characterised by high values of equivalent potential temperature (up to 320 K (not shown) were advected from southeastern Europe into eastern Germany resulting in unstable conditions (SLI values between -2 and -6 K; Fig. 8a) and high atmospheric moisture content (PW values between 25 and 40 kg m^{-2} ; Fig. 8b), which are both conducive to widespread thunderstorm formation (cf. Greene and Clark 1972; Manzato 2003; Kunz 2007; Mohr 2013). Additionally, the squall line developed in front of a cold front approaching from the west (not shown) in a region with strong lifting (OMEGA values up to 40 hPa/h at 12 UTC in northwestern Germany; Fig. 8c). These conditions favoured and promoted the formation of deep moist convection. Several studies have already demonstrated the role of cold fronts for the initiation of severe convection mainly due to lifting and wind shear (Heymsfield and Schotz 1985; Doswell 1987; Schemm *et al.* 2016; Kunz *et al.* 2019). Thus, the three major requirements for the formation of deep moist convection, ie., (1) a high moisture content in the lower troposphere, (2) thermal instability of the atmosphere and (3) a trigger mechanism were fulfilled (Doswell 1987).

This contrasts with the conditions prevailing on 19 June 2001 for blocking in the NA area (Fig. 7 bottom), where no thunderstorms occurred (Fig. 7d). On that day, a northerly mid-tropospheric flow was present over the investigation area due to an upper-level ridge over the eastern North Atlantic and the blocking anticyclone (not shown). This situation resulted in dry ($\text{PW} < 20 \text{ kg m}^{-2}$; Fig. 8e) and stable ($\text{SLI} > 0 \text{ K}$; Fig. 8d) and, thus, convection-inhibiting conditions over western and central Europe (cf. Doswell 1987; Piper *et al.* 2019). Furthermore, the large-scale subsidence was present over most parts of the investigation area ($\text{OMEGA} < 15 \text{ hPa/h}$; Fig. 8f).

In the next step, the environmental conditions during blocking in BS and NA areas are analysed statistically to examine whether the mechanisms described in the previous Section are representative for a larger sample.

In doing so, we investigate 371 (BS) and 373 (NA) blocking days/events during the investigation period between 2001 and 2014. Anomaly composites (Fig. 9) are prepared for these two event sets by calculating the mean deviation from the climatology of the considered variable (reference period: 1981 – 2010, May to August) including its statistical significance (cf. Sec. 2.4). Because anomaly composites of Φ_{500} (and PV) primarily reflect the block position (not shown), these are not explicitly presented.

For cases of blocking in the BS area (Fig. 9 left), the results of the case study above are confirmed with regards to lower stability and increased moisture of the air masses in the investigation area than on average (Fig. 9a,b). SLI anomaly values between -0.5 and -1.5 K and higher PW values between 1 and 4 kg m^{-2} are observed in the investigation area, with the deviation from the climatological mean is also statistically significant (Fig. 9 black dots). For both parameters the anomalies are not only evident on the regional scale, but also representative and significant for a large area of western and central Europe. Regarding large-scale vertical wind, however, the signals from OMEGA are on average not conspicuous or differentiating (Fig. 9c).

Furthermore, it appears that during blocking in the BS area the air masses in the lower troposphere (850 to 700 hPa) relevant to the thunderstorm development are mainly transported from the North Atlantic and along the Iberian Peninsula from the Mediterranean Sea and sometimes and also from the East (not shown).

Transport from the East is observed in particular in connection with thunderstorms in Germany, but less in France. Similar results are reported by Busch (2013) for selected (large) hail events and by Graf *et al.* (2011) for tornadoes in Europe. For example, Busch (2013) found with a Lagrangian method based on backward trajectories that mainly air mass transport from the North Atlantic takes place. Especially in central Europe, air masses leading to hail mainly originate from western regions (Atlantic origin) or from the continental regions of Eastern Europe. In addition, isolated trajectories also started in the Mediterranean region and flowed around the Alps. With the same method Graf *et al.* (2011) observed that most low-level backward trajectories of European tornadoes started over the Atlantic Ocean, whereas some events are

also related with Mediterranean air. Trefalt *et al.* (2018) also studied moisture sources for a hailstorm in northern Switzerland and identify the Mediterranean and local sources as main moisture sources.

During blocking in the NA area, large-scale subsidence occurs on average over most of the investigation area. This applies in particular to France, Switzerland, Benelux and southern and northwestern Germany (significant in Fig. 9f). Furthermore, air masses are more stable (significant anomalies up to 2 K; Fig. 9d) with SLI values on average between 0 and 4 K on those days. Moreover, the air masses are drier compared to the climatological average (Fig. 9e). These results are in turn statistically significant for a spatially extended area.

Additionally, we investigate DLS during both blocking situations because high DLS values are often related to severe convective weather like (large) hail, severe wind gusts, or tornado in Europe (Brooks *et al.* 2003; Púčik *et al.* 2015; Rädler *et al.* 2018; Kunz *et al.* 2019). Strong vertical wind shear enables longer storm lifetime, supports organised convective systems, and, thus, storm severity (Markowski and Richardson 2010). During both blocking situations, DLS values over the investigation area are lower by up to 3 m s^{-1} than in the climatological mean (blue in Fig. 10). For comparison, the values of the climatological mean are between 6 and 11 m s^{-1} for the investigation area (not shown). The standard deviation of 6 to 7 m s^{-1} is relatively large and indicates a high temporal variability (not shown). Most of the blocks in the BS area are associated with lower DLS values in the investigation area (e.g., $\text{DLS} < 15 \text{ m s}^{-1}$ around 80%). Similar wind conditions were also observed in two studies investigating heavy precipitation in Germany in 2016 and 2018 accompanied by atmospheric blocking over Northern Europe (Piper *et al.* 2016; Mohr *et al.* 2019). Note, however, that ERA-Interim (and reanalyses overall) may have a tendency to underestimate vertical wind shear (Taszarek *et al.* 2018). In addition, we observe individual days, during which high DLS values between 20 and 30 m s^{-1} are found (around 10% of the blocking days in BS area). An example is the case presented in Figure 7 (cf. Sec. 5.1), where high DLS between 17 and 30 m s^{-1} over France supported the occurrence of an organised squall line (not shown).

The reason for the different signals related to DLS during blocking is due to the synoptic scale flow: the varying location of the western flank of the blocking ridge associated with troughs and fronts upstream. For example, Rossby wave breaking is one relevant process for the blocking occurrence and, thus, for the position of blocking and the resulting mid-tropospheric flow (Masato *et al.* 2012; Quinting and Vitart 2019). Visual analyses identify two different preferred flow situations during blocking in the BS area: The first one

Accepted Article

is a typical Omega block (usual situation), where the investigation area is below the block associated with a ridge, where typically low DLS values are found. Piper *et al.* (2019, their Fig. 2) also observed convective cases, where regions located below a ridge are frequently characterised by a lack of large-scale lifting. In the second situation, the identified block has a smaller wavelength and is connected to a cyclonically tilted ridge, so that the investigation area may be influenced by an upstream trough with higher wind speeds in the mid-troposphere. Overall, this finding confirms that blocking in the BS area leads on average to less organised thunderstorms, but can also be associated with high shear conditions in individual cases assisting the formation of severe (organised) convective storms.

Finally, we carry out our analyses for the sub-areas defined in Figure 4. By a shift of the blocking area from west to east for both the NA and BS area, the flow situation and the resulting air mass transport are also shifted, which in turn leads, for example in the case of atmospheric stability (SLI), to a shift of the regions with unstable (or stable) air masses from west to east (not shown). The same relationships are found for the other investigated meteorological parameters. This result explains the shift of the high OR values from west to east in Figure 5.

6. Summary and conclusions

This study examines the link between atmospheric blocking over the eastern North Atlantic and northern Europe and thunderstorm activity in western and central Europe. In addition, we show how blocking modulates relevant atmospheric mechanisms that support or suppress the development of convective storms. We used the ERA-Interim reanalysis to identify blocking systems (following the method of Schierz *et al.* 2004) and to study atmospheric conditions prevailing during days with blocking for the time period between 2001 and 2014. First, the location of relevant areas, where blocking influences thunderstorm activity (based on lightning data) were identified. Second, the link between blocking at these locations and thunderstorm days was determined using logistic regression models (odds ratio). Third, anomaly composites of several meteorological parameters describing, for example, prevailing atmospheric stability, flow situation, or moisture content of the air masses were constructed to study the physical mechanisms behind the statistical links.

The following major findings and conclusions are inferred from the obtained results:

1. Two regimes were identified, where blocking significantly affects the probability of thunderstorm days over western and central Europe. One is located over the eastern part of the North Atlantic (convection-inhibiting conditions) and one over the Baltic Sea (convection-favouring conditions). Blocking in the North Atlantic area mainly affects thunderstorm frequency in the central and northeastern part of France, while blocking over the Baltic Sea mainly affects thunderstorm activity in northern Germany.
2. For both areas, approximately 22 % of the days between May and August are identified as blocking days (20 % of the defined area has to be covered by a block signal). In the North Atlantic area, blocking is most frequent in May and June, whereas blocking over the Baltic Sea peaks in July. Furthermore, blocking in both areas exhibits a high year-to-year variability, which could explain part of the high annual variability of thunderstorms or hail days in Europe.
3. Based on the mean environmental conditions during days with blocking, some relevant dynamic and thermodynamic mechanisms can be confirmed that support or suppress the development of thunderstorm activity. The anticyclonic circulation of a blocking ridge over the eastern part of the North Atlantic leads in northerly to northwesterly advection of dry and stable air masses on the eastern flank of the block. In addition, the large-scale environmental conditions are on average associated with a large-scale subsidence of air masses (convection-inhibiting conditions). In contrast, the southerly to southwesterly advection of warm, moist and unstable air masses (mainly from Atlantic, but sometimes also from the Mediterranean or Eastern region) on the western flank of a blocking system over the Baltic Sea results in preferably convection-favouring conditions.
4. The two blocking situations are on average connected with weak wind speeds at mid-troposphere levels and hence weak wind shear over the investigation area. As a consequence, thunderstorms during atmospheric blocking over the Baltic Sea might be on average less organised. However, days with high wind shear values between 20 and 30 m s⁻¹ are also observed during blocking over the Baltic Sea (around 10 %). The shape of the blocking systems and the different position of the upstream trough in relation to the area where thunderstorms occur explain the two different shear situations.

In summary, our study demonstrates that atmospheric blocking over the North Atlantic and the Baltic Sea has remote effects on deep moist convection in western and central Europe. This supports the statement of Piper *et al.* (2019) that convective predisposition is decisively influenced by the state of mid-tropospheric

flow steering the large-scale thermodynamic and dynamic conditions relevant for convection. Flow patterns, for example, associated with advection of warm air masses at low levels from southwesterly regions from Spain to France and central Europe in combination with an elevated mixed layer (Carlson *et al.* 1983; Lanicci and Warner 1991) and a Spanish plume event (Morris 1986; van Delden 2001; Piper 2017) often produce a conducive environment for the development of (severe) thunderstorms (Kunz *et al.* 2018; Piper *et al.* 2019).

With respect to blocking over the Baltic Sea, the correlation to thunderstorm occurrence seems to be more relevant in regions where convection is often related to synoptic forcing like cold fronts such as in the middle of France, northern Germany, or south of the Alps in Switzerland (Schemm *et al.* 2016; Kunz *et al.* 2019) compared to regions with local-scale forcing dominated by orographic effects (Morel and Senesi 2002; Barthlott *et al.* 2011) such as southern Germany or eastern Austria.

A comparison of our results with a study regarding an extended definition of seven North Atlantic-European weather regimes (Grams *et al.* 2017) shows that a block in the NA area is similar to the weather regime called *Atlantic ridge* and a block in the Baltic Sea areas to the regime *Scandinavian blocking*. The weather regime *European blocking* of that study represents the crossover cases, where blocking exists simultaneously in both areas. These three regimes are observed during the summer on 30–35 % of all days (see supplementary of Grams *et al.* 2017).

In contrast to other approaches such as considering teleconnection patterns (cf. Allen *et al.* 2015; Tippett *et al.* 2015; Piper and Kunz 2017; Trapp and Hoogewind 2018; Piper *et al.* 2019), regions with blocking establish direct links to dynamic and thermodynamic mechanisms and processes influencing the thunderstorm formation. The location of the relevant (influencing) areas was determined in this study itself, whereas teleconnection patterns are already defined for a predefined area. In contrast to teleconnection patterns, which capture the annual variability, atmospheric blocking affects the prevailing (stationary) environmental conditions such as atmospheric stability and moisture content of air masses. Nevertheless, blocking is not suitable as a single predictor for convection; here, other approaches should be pursued (cf. Doswell *et al.* 1996; Sánchez *et al.* 2009; Mohr *et al.* 2015b; Púčik *et al.* 2015; Rädler *et al.* 2018). Due to its persistence, blocking might contribute to improved thunderstorm potential predictability on sub-seasonal time scales beyond the classical weather forecast time scale of a few days and complement current activities that investigate the connection of water vapour transport on the sub-seasonal predictability

of extremes (e.g., Lavers *et al.* 2016a,b; Pasquier *et al.* 2018). It is important, however, that—especially in connection with local-scale phenomena such as deep moist convection—the blocking position is correctly predicted, which is currently still a challenge in state-of-the-art global numerical weather prediction models (Quinting and Vitart 2019).

Acknowledgement

This work results from a visiting researcher's stay at the University of Bern. First of all, the first author would like to thank everyone who made this possible. Furthermore, the authors thank the BLitz InformationDienst Siemens (BLIDS), namely Stefan Thern for providing and David Piper for post-processing lightning data. Further, we thank the European Centre for Medium-Range Weather Forecasts (ECMWF) for providing the ERA-Interim data. Additionally, the first author acknowledges the helpful discussions with Christian Grams, Michael Kunz, and Julian Quinting. Data are stored at the Research Data Archive at the Karlsruhe Institute of Technology (KIT) and can be made available upon request to the first author. OM and SL acknowledge support from the Swiss Science Foundation Grant Number 200021_156059. We acknowledge the constructive comments from two anonymous reviewers, which helped to improve the quality of the article.

References

- Alfonso JT, Tippett MK, Sobel AH. 2015. Influence of the El Niño/Southern Oscillation on tornado and hail frequency in the United States. *Nat. Geosci.* **8**: 278–283, doi:10.1038/ngeo2385.
- Anderson G, Klugmann D. 2014. A European lightning density analysis using 5 years of ATDnet data. *Nat. Hazards Earth Syst. Sci.* **14**: 815–829, doi:10.5194/nhess-14-815-2014.
- Balkhaus K, Erichson B, Plinke W, Weiber R. 2016. *Multivariate Analysemethoden: eine anwendungsorientierte Einführung*. Springer-Verlag, Heidelberg, Germany.
- Giopetro D, García-Herrera R, Lupo AR, Hernández E. 2006. A climatology of Northern Hemisphere blocking. *J. Climate* **19**: 1042–1063, doi:10.1175/JCLI3678.1.
- Baehlott C, Burton R, Kirshbaum D, Hanley K, Richard E, Chaboureau JP, Trentmann J, Kern B, Bauer HS, Schwitalla T, *et al.* 2011. Initiation of deep convection at marginal instability in an ensemble of mesoscale models: A case-study from COPS. *Q. J. R. Meteorol. Soc.* **137**: 118–136, doi:10.1002/qj.707.
- Bertram I, Mayr GJ. 2004. Lightning in the eastern Alps 1993–1999, Part I: Thunderstorm tracks. *Nat. Hazards Earth Syst. Sci.* **4**: 501–511, doi:10.5194/nhess-4-501-2004.
- Bieli M, Pfahl S, Wernli H. 2015. A Lagrangian investigation of hot and cold temperature extremes in Europe. *Q. J. R. Meteorol. Soc.* **141**: 98–108, doi:10.1002/qj.2339.
- Brooks HE, Lee JW, Craven JP. 2003. The spatial distribution of severe thunderstorm and tornado environments from global reanalysis data. *Atmos. Res.* **67**: 73–94, doi:10.1016/S0169-8095(03)00045-0.
- Brunner L, Schaller N, Anstey J, Sillmann J, Steiner AK. 2018. Dependence of present and future European temperature extremes on the location of atmospheric blocking. *Geophys. Res. Lett.* **45**: 6311–6320, doi:10.1029/2018gl077837.

- Busch M. 2013. Untersuchung der Luftmasseigenschaften und ihrer Transformation bei schweren Hagelereignissen über Europa. Master's thesis, Institute for Meteorology and Climate Research (IMK), Karlsruhe Institute of Technology (KIT), Germany. Available from: <http://occrdata.unibe.ch/students/theses/msc/229.pdf> [Accessed 13-Mai-2019].
- Carlson TN, Benjamin SG, Forbes GS, Li YF. 1983. Elevated mixed layers in the regional severe storm environment: Conceptual model and case studies. *Mon. Weather Rev.* **111**: 1453–1474, doi:10.1175/1520-0493(1983)111<1453:EMLITR>2.0.CO;2.
- Croci-Maspoli M, Schwierz C, Davies HC. 2007. A multi-faceted climatology of atmospheric blocking and its recent linear trend. *J. Climate* **20**: 633–649, doi:10.1175/JCLI4029.1.
- Dee DP, Uppala SM, Simmons AJ, Berrisford P, Poli P, Kobayashi S, Andrae U, Balmaseda MA, Balsamo G, Bauer P, Bechtold P, Beljaars ACM, Van De Berg L, Bidlot J, Bormann N, Delsol C, Dragani R, Fuentes M, Geer AJ, Haimberger L, Healy SB, Hersbach H, Hólm EV, Isaksen L, Kållberg P, Köhler M, Matricardi M, McNally AP, Monge-Sanz BM, Morcrette JJ, Park BK, Peubey C, De Rosnay P, Tavalato C, Thépaut JN, Vitart F. 2011. The ERA-Interim reanalysis: Configuration and performance of the data assimilation system. *Q. J. R. Meteorol. Soc.* **137**: 553–597, doi:10.1002/qj.828.
- Doswell CA. 1987. The distinction between large-scale and mesoscale contribution to severe convection: A case study example. *Weather Forecast.* **2**: 3–16, doi:10.1175/1520-0434(1987)002<0003:TDBLSA>2.0.CO;2.
- Doswell CA, Brooks HE, Maddox RA. 1996. Flash flood forecasting: An ingredients-based methodology. *Weather Forecast.* **11**: 560–581, doi:10.1175/1520-0434(1996)011<0560:FFFAIB>2.0.CO;2.
- Drüe C, Hauf T, Finke U, Keyn S, Kreyer O. 2007. Comparison of a SAFIR lightning detection network in northern Germany to the operational BLIDS network. *J. Geophys. Res. Atmos.* **112**: D18 114, doi:10.1029/2006JD007680.
- Finke U, Hauf T. 1996. The characteristics of lightning occurrence in southern Germany. *Beitr. Phys. Atmosph.* **69**: 361–374.
- Gatzen C. 2004. A derecho in Europe: Berlin, 10 July 2002. *Weather Forecast.* **19**: 639–645, doi:10.1175/1520-0434(2004)019<0639:ADIEBJ>2.0.CO;2.
- Graf MA, Sprenger M, Moore RW. 2011. Central European tornado environments as viewed from a potential vorticity and Lagrangian perspective. *Atmos. Res.* **101**: 31–45, doi:10.1016/j.atmosres.2011.01.007.
- Grams CM, Beerli R, Pfenninger S, Staffell I, Wernli H. 2017. Balancing Europe's wind-power output through spatial deployment informed by weather regimes. *Nat. Clim. Change* **7**: 557, doi:10.1038/nclimate3338.
- Grams CM, Binder H, Pfahl S, Piaget N, Wernli H. 2014. Atmospheric processes triggering the central European floods in June 2013. *Nat. Hazards Earth Syst. Sci.* **14**: 1691–1702, doi:10.5194/nhess-14-1691-2014.
- Greene DR, Clark RA. 1972. Vertically integrated liquid water – A new analysis tool. *Mon. Weather Rev.* **100**: 548–552, doi:10.1175/1520-0493(1972)100<0548:VILWNA>2.3.CO;2.
- Halander AJ, van Delden A. 2003. Thunderstorm predictors and their forecast skill for the Netherlands. *Atmos. Res.* **67–68**: 273–299, doi:10.1016/S0169-8095(03)00056-5.
- Hemsfield GM, Schotz S. 1985. Structure and evolution of a severe squall line over Oklahoma. *Mon. Weather Rev.* **113**: 1563–1589, doi:10.1175/1520-0493(1985)113<1563:SAEOAS>2.0.CO;2.
- Hong CC, Hsu HH, Lin NH, Chiu H. 2011. Roles of European blocking and tropical-extratropical interaction in the 2010 Pakistan flooding. *Geophys. Res. Lett.* **38**, doi:10.1029/2011GL047583.
- Kaltenböck R, Diendorfer G, Dotzek N. 2009. Evaluation of thunderstorm indices from ECMWF analyses, lightning data and severe storm reports. *Atmos. Res.* **93**: 381–396, doi:10.1016/j.atmosres.2008.11.005.
- Kunsch ML, Kunz M, Vitolo R, Economou T. 2012. Long-term trends of hail-related weather types in an ensemble of regional climate models using a Bayesian approach. *J. Geophys. Res.* **117**(D15107), doi:10.1029/2011JD017185.
- Kunz M. 2007. The skill of convective parameters and indices to predict isolated and severe thunderstorms. *Nat. Hazards Earth Syst. Sci.* **7**: 327–342, doi:10.5194/nhess-7-327-2007.
- Kunz M, Blahak U, Handwerker J, Schmidberger M, Punge H J, Mohr S, Fluck E, Bedka K M. 2018. The severe hailstorm in Germany on 28 July 2013: Characteristics, impacts, and meteorological conditions. *Q. J. R. Meteorol. Soc.* **144**: 231–250, doi:10.1002/qj.3197.
- Kunz M, Sander J, Kottmeier C. 2009. Recent trends of thunderstorm and hailstorm frequency and their relation to atmospheric characteristics in southwest Germany. *Int. J. Climatol.* **29**: 2283–2297, doi:10.1002/joc.1865.
- Kunz M, Wandel J, Fluck E, Baumstark S, Mohr S, Schemm S. 2019. Ambient conditions prevailing during hail events estimated from a combination of radar data and observations in central Europe. *Q. J. R. Meteorol. Soc.*, in review .
- Lanucci JM, Warner TT. 1991. A synoptic climatology of the elevated mixed-layer inversion over the southern Great Plains in spring. Part I: Structure, dynamics, and seasonal evolution. *Weather Forecast.* **6**: 181–197, doi:10.1175/1520-0434(1991)006<0181:ASCOTE>2.0.CO;2.

- Lavers DA, Pappenberger F, Richardson DS, Zsoter E. 2016a. ECMWF Extreme Forecast Index for water vapor transport: A forecast tool for atmospheric rivers and extreme precipitation. *Geophys. Res. Lett.* **43**: 11,852–11,858, doi:10.1002/2016GL071320.
- Lavers DA, Waliser DE, Ralph FM, Dettinger MD. 2016b. Predictability of horizontal water vapor transport relative to precipitation: Enhancing situational awareness for forecasting western US extreme precipitation and flooding. *Geophys. Res. Lett.* **43**: 2275–2282, doi:10.1002/2016GL067765.
- Lenggenhager S, Croci-Maspoli M, Brönnimann S, Martius O. 2018. On the dynamical coupling between atmospheric blocks and heavy precipitation events: A discussion of the southern Alpine flood in October 2000. *Q. J. R. Meteorol. Soc.* **145**: 530–545, doi:10.1002/qj.3449.
- Lenggenhager S, Martius O. 2019. Atmospheric blocks modulate the odds of heavy precipitation events in Europe. *Clim. Dynam.* doi:10.1007/s00382-019-04779-0.
- Madonna E, Ginsbourger D, Martius O. 2018. A Poisson regression approach to model monthly hail occurrence in Northern Switzerland using large-scale environmental variables. *Atmos. Res.* **203**: 261–274, doi:10.1016/j.atmosres.2017.11.024.
- Mählstein I, Martius O, Chevalier C, Ginsbourger D. 2012. Changes in the odds of extreme events in the Atlantic basin depending on the position of the extratropical jet. *Geophys. Res. Lett.* **39**: L22 805, doi:10.1029/2012GL053993.
- Manzato A. 2003. A climatology of instability indices derived from Friuli Venezia Giulia soundings, using three different methods. *Atmos. Res.* **67**: 417–454, doi:10.1016/S0169-8095(03)00058-9.
- Markowski P, Richardson Y. 2010. *Mesoscale meteorology in midlatitudes*. John Wiley & Sons, Chichester, UK.
- Martius O, Sodemann H, Joos H, Pfahl S, Winschall A, Croci-Maspoli M, Graf M, Madonna E, Mueller B, Schemm S, Sedlacek J, Sprenger M, Wernli H. 2013. The role of upper-level dynamics and surface processes for the Pakistan flood of July 2010. *Q. J. R. Meteorol. Soc.* **139**: 1780–1797, doi:10.1002/qj.2082.
- Masato G, Hoskins BJ, Woollings TJ. 2012. Wave-breaking characteristics of midlatitude blocking. *Q. J. R. Meteorol. Soc.* **138**: 1285–1296, doi:10.1002/qj.990.
- Merino A, Sánchez JL, Fernández-González S, García-Ortega E, Marcos JL, Berthet C, Dessens J. 2019. Hailfalls in southwest Europe: EOF analysis for identifying synoptic pattern and their trends. *Atmos. Res.* **215**: 42–56, doi:10.1016/j.atmosres.2018.08.006.
- Merino A, Wu X, Gascón E, Berthet C, García-Ortega E, Dessens J. 2014. Hailstorms in southwestern France: Incidence and atmospheric characterization. *Atmos. Res.* **140–141**: 61–75, doi:10.1016/j.atmosres.2014.01.015.
- Mohr S. 2013. Änderung des Gewitter- und Hagelpotentials im Klimawandel. PhD thesis, Wiss. Berichte d. Instituts für Meteorologie und Klimaforschung des Karlsruher Instituts für Technologie, Vol. 58, KIT Scientific Publishing, Karlsruhe, Germany, doi:10.5445/KSP/1000033828.
- Mohr S, Kunz M. 2013. Recent trends and variabilities of convective parameters relevant for hail events in Germany and Europe. *Atmos. Res.* **123**: 211–228, doi:10.1016/j.atmosres.2012.05.016.
- Mohr S, Kunz M, Geyer B. 2015a. Hail potential in Europe based on a regional climate model hindcast. *Geophys. Res. Lett.* **42**: 10904–10912, doi:10.1002/2015GL067118.
- Mohr S, Kunz M, Keuler K. 2015b. Development and application of a logistic model to estimate the past and future hail potential in Germany. *J. Geophys. Res.* **120**: 3939–3956, doi:10.1002/2014JD022959.
- Mohr S, Wandel J, Wilhelm J, Kunz M, Portman R, Punge H J, Schmidberger M, Grams C. 2019. The role of large-scale dynamics in an exceptional sequence of severe thunderstorms in Europe. *J. Geophys. Res. Atmos., in review*.
- Morel C, Senesi S. 2002. A climatology of mesoscale convective systems over Europe using satellite infrared imagery. II: Characteristics of European mesoscale convective systems. *Q. J. R. Meteorol. Soc.* **128**: 1973–1995, doi:10.1256/003590002320603494.
- Morris RM. 1986. The spanish plume-testing the forecasters nerve. *Meteorol. Mag.* **115**: 349–357.
- Müller L, Martius O, Hering A, Kunz M, Germann U. 2016. Spatial and temporal distribution of hailstorms in the Alpine region: a long-term, high resolution, radar-based analysis. *Q. J. R. Meteorol. Soc.* **142**: 1590–1604, doi:10.1002/qj.2771.
- Pasquier JT, Pfahl S, Grams C. 2018. Modulation of atmospheric rivers and associated precipitation extremes in the North Atlantic region by European weather regimes. *Geophys. Res. Lett.* **46**: 1014–1023, doi:10.1029/2018GL081194.
- Pfahl S, Wernli H. 2012. Quantifying the relevance of atmospheric blocking for co-located temperature extremes in the Northern Hemisphere on (sub-)daily time scales. *Geophys. Res. Lett.* **39**: L12 807, doi:10.1029/2012GL052261.
- Piper D. 2017. Untersuchung der Gewitteraktivität und der relevanten großräumigen Steuerungsmechanismen über Mittel- und Westeuropa. PhD thesis, Wiss. Berichte d. Instituts für Meteorologie und Klimaforschung des Karlsruher Instituts für Technologie, Vol. 73, KIT Scientific Publishing, Karlsruhe, Germany, doi:10.5445/KSP/1000072089.
- Piper D, Kunz M. 2017. Spatiotemporal variability of lightning activity in Europe and the relation to the North Atlantic Oscillation teleconnection pattern. *Nat. Hazards Earth Syst. Sci.* **17**: 1319–1336, doi:10.5194/nhess-17-1319-2017.

- Piper D, Kunz M, Allen J, Mohr S. 2019. Temporal variability of thunderstorms in Central and Western Europe is driven by large-scale flow and teleconnection patterns. *Q. J. R. Meteorol. Soc.*, in review .
- Piper D, Kunz M, Ehmele F, Mohr S, Mühr B, Kron A, Daniell J. 2016. Exceptional sequence of severe thunderstorms and related flash floods in May and June 2016 in Germany. Part I: Meteorological background. *Nat. Hazards Earth Syst. Sci.* **16**: 2835–2850, doi:10.5194/nhess-16-2835-2016.
- Poelman DR, Schulz W, Diendorfer G, Bernardi M. 2016. The European lightning location system EUCLID – Part 2: Observations. *Nat. Hazards Earth Syst. Sci.* **16**: 607–616, doi:10.5194/nhess-16-607-2016,2016.
- Pučík T, Groenemeijer P, Rýva D, Kolář M. 2015. Proximity soundings of severe and nonsevere thunderstorms in Central Europe. *Mon. Weather Rev.* **143**: 4805–4821, doi:10.1175/MWR-D-15-0104.1.
- Quandt LA, Keller JH, Martius O, Jones SC. 2017. Forecast variability of the blocking system over Russia in summer 2010 and its impact on surface conditions. *Weather Forecast.* **32**: 61–82, doi:10.1175/WAF-D-16-0065.1.
- Reuter JF, Vitart F. 2019. Representation of synoptic-scale Rossby wave packets and blocking in the S2S Prediction Project Database. *Geophys. Res. Lett.* **46**: 1070–1078, doi:10.1029/2018GL081381.
- Riederer AT, Groenemeijer P, Faust E, Sausen R. 2018. Detecting severe weather trends using an Additive Regressive Convective Hazard Model (AR-CHaMo). *J. Appl. Meteorol. Climatol.* **57**: 569–587, doi:10.1175/JAMC-D-17-0132.1.
- Rex DF. 1950a. Blocking action in the middle troposphere and its effect upon regional climate: I. An aerological study of blocking action. *Tellus* **2**: 196–211, doi:10.3402/tellusa.v2i4.8603.
- Rex DF. 1950b. Blocking action in the middle troposphere and its effect upon regional climate: II. The climatology of blocking action. *Tellus* **2**: 275–301, doi:10.3402/tellusa.v2i4.8603.
- Röthlisberger M, Martius O, Wernli H. 2018. Northern Hemisphere Rossby wave initiation events on the extratropical jet – A climatological analysis. *J. Climate* **31**: 743–760, doi:10.1175/JCLI-D-17-0346.1.
- Sánchez JL, Marcos JL, Dessens J, López L, Bustos C, García-Ortega E. 2009. Assessing sounding-derived parameters as storm predictors in different latitudes. *J. Atmos. Res.* **93**: 446–456, doi:10.1016/j.atmosres.2008.11.006.
- Santos JA, Belo-Pereira M. 2019. A comprehensive analysis of hail events in Portugal: Climatology and consistency with atmospheric circulation. *Int. J. Climatol.* **39**: 188–205, doi:10.1002/joc.5794.
- Schemm S, Luca N, Martinov A, Leuenberger D, Martius O. 2016. On the link between cold fronts and hail in Switzerland. *Atmos. Sci. Lett.* **5**: 315–325, doi:10.1002/asl.660.
- Scherrer SC, Croci-Maspoli M, Schwierz C, Appenzeller C. 2006. Two-dimensional indices of atmospheric blocking and their statistical relationship with winter climate patterns in the Euro-Atlantic region. *Int. J. Climatol.* **26**: 233–249, doi:10.1002/joc.1250.
- Schroeder K, Kunz M, Elmer F, Mühr B, Merz B. 2015. What made the June 2013 flood in Germany an exceptional event? A hydro-meteorological evaluation. *Hydrol. Earth Syst. Sci.* **19**: 309–327, doi:10.5194/hess-19-309-2015,2015.
- Schulz W, Diendorfer G, Pedeboy S, Poelman DR. 2016. The European lightning location system EUCLID – Part 1: Performance analysis and validation. *Nat. Hazards Earth Syst. Sci.* **16**: 595–605, doi:10.5194/nhess-16-595-2016.
- Schwierz C, Croci-Maspoli M, Davies HC. 2004. Perspicacious indicators of atmospheric blocking. *Geophys. Res. Lett.* **31**: L06125, doi:10.1029/2003GL019341.
- Sillmann J, Croci-Maspoli M. 2009. Present and future atmospheric blocking and its impact on European mean and extreme climate. *Geophys. Res. Lett.* **36**: L07702, doi:10.1029/2009GL038259.
- Sillmann J, Croci-Maspoli M, Kallache M, Katz RW. 2011. Extreme cold winter temperatures in Europe under the influence of North Atlantic atmospheric blocking. *J. Climate* **24**: 5899–5913, doi:10.1175/2011JCLI4075.1.
- Sousa PM, Trigo RM, Barriopedro D, Soares PMM, Ramos AM, Liberato MLR. 2017. Responses of European precipitation distributions and regimes to different blocking locations. *Clim. Dynam.* **48**: 1141–1160, doi:10.1007/s00382-016-3132-5.
- Sousa PM, Trigo RM, Barriopedro D, Soares PMM, Santos JA. 2018. European temperature responses to blocking and ridge regional patterns. *Clim. Dynam.* **50**: 457–477, doi:10.1007/s00382-017-3620-2.
- Taszarek M, Allen JT, Pučík T, Groenemeijer P, Czernecki B, Kolendowicz L, Lagouvardos K, Kotroni V, Schulz W. 2019. A climatology of thunderstorms across Europe from a synthesis of multiple data sources. *J. Climate* **32**: 1813–1837, doi:10.1175/JCLI-D-18-0372.1.
- Taszarek M, Brooks HE, Czernecki B. 2017. Sounding-derived parameters associated with convective hazards in Europe. *Mon. Weather Rev.* **145**: 1511–1528, doi:10.1175/MWR-D-16-0384.1.

- Taszarek M, Brooks HE, Czernecki B, Szuster P, Fortuniak K. 2018. Climatological aspects of convective parameters over Europe: A comparison of ERA-Interim and sounding data. *J. Climate* **31**: 4281–4308, doi:10.1175/JCLI-D-17-0596.1.
- Tippett MK, Allen JT, Gensini VA, Brooks HE. 2015. Climate and hazardous convective weather. *Curr. Clim. Change Rep.* **1**: 60–73, doi:10.1007/s40641-015-0006-6.
- Trapp RJ, Hoogewind KA. 2018. Exploring a possible connection between US tornado activity and Arctic sea ice. *npj Clim. Atmos. Sci.* **1**: 14, doi:10.1038/s41612-018-0025-9.
- Trefalt S, Martynov A, Barras H, Besic N, Hering AM, Lenggenhager S, Noti P, Rothlisberger M, Schemm S, Germann U, Martius O. 2018. A severe hail storm in complex topography in Switzerland – Observations and processes. *Atmos. Res.* **209**: 76–94, doi:10.1016/j.atmosres.2018.03.007.
- Truesherth KE, Fasullo JT. 2012. Climate extremes and climate change: The Russian heat wave and other climate extremes of 2010. *J. Geophys. Res.* **117**: D17103, doi:10.1029/2012JD018020.
- Uhlenbrock D, Delden A. 2001. The synoptic setting of thunderstorms in Western Europe. *Atmos. Res.* **56**: 89–110, doi:10.1016/S0169-8095(00)00092-2.
- Villiger L. 2017. Block detection and European heat waves. Master's thesis, Faculty of Sciences, University of Bern, Bern, Switzerland. Available from: <http://occrdata.unibe.ch/students/theses/msc/229.pdf> [Accessed 13-May-2019].
- Wapler K. 2013. High-resolution climatology of lightning characteristics within Central Europe. *Meteorol. Atmos. Phys.* **122**: 175–184, doi:10.1007/s00703-013-0285-1.
- Wapler K, James P. 2015. Thunderstorm occurrence and characteristics in Central Europe under different synoptic conditions. *Atmos. Res.* **158**: 231–244, doi:10.1016/j.atmosres.2014.07.011.
- Westerreicher AT, Groenemeijer P, Pistotnik G, Sausen R, Faust E. 2016. Identification of favorable environments for thunderstorms in reanalysis data. *Meteorol. Z.* **26**: 59–70, doi:10.1127/metz/2016/0754.
- Webbings T, Barriopedro D, Methven J, Son SW, Martius O, Harvey B, Sillmann J, Lupo AR, Seneviratne S. 2018. Blocking and its response to climate change. *Curr. Clim. Change Rep.* **4**: 287–300, doi:10.1007/s40641-018-0108-z.

Captions

Table 1: Annual number per year (left) and annual mean per month including standard deviation (right) of blocking events in the two areas NA and BS (cf. Fig. 5) during the investigation period.

Fig. 1: Mean annual number of thunderstorm days during May to August between 2001 and 2014 (FR = France, BE = Belgium, NE = Netherlands, LU = Luxembourg, GE = Germany, CH = Switzerland, AT = Austria,); the black line indicates the contiguous area of the 132 GPs referred to as FOCREG (see Chap. 3).

Fig. 2: Relative blocking frequency between 2001 and 2014 (May – August).

Fig. 3: Two examples of identified areas with statistically significant (p-value at 95 % significance level) changes in the odds ratio, where blocking affects the thunderstorm activity in two reference regions: (a) 48°N 4°E and (b) 52°N 11°E (illustrated as orange grid point). The blue colours indicate a reduction of thunderstorm days by blocking (e.g., a value of 0.5 means a decrease of the odds by 50 %) and red colours indicate an increase (e.g., a value of 2 means a doubling of the odds).

Fig. 4: Relative frequency of the 132 OR calculations quantifying how often (a) $OR < 1$ (blocking suppresses TDs; blue in Fig. 3) or (b) $OR > 1$ (blocking supports TDs; red in Fig. 3). The black lines indicate the threshold₁ with 40 %. The numbers define the sub-areas over the North Atlantic (1 = West and 2 = East) and the Baltic Sea (3 = West and 4 = East) for further investigations.

Fig. 5: Same as Fig. 3; but for the six areas (defined in Fig. 4): (a-c) North Atlantic (NA) and (d-f) Baltic Sea (BS) with their respective sub-areas (b) NA West & (c) NA East and (e) BS West & (f) BS East. Note only values with a OR with p-value of at least 95 % significance level are shown.

Fig. 6: Same as Fig. 3; but for the crossover cases. Shown are (a) changes in the odds ratio at every grid point and (b) only grid points with statistically significant values (p-value at 95 % significance level).

Fig. 7 Examples of blocking events on 10 July 2002 over the NA (top) and on 19 June 2001 over the BS (bottom): (a,c) Φ_{500} in gpm with blocks (grey contour) and (b,d) thunderstorm day (yes in beige).

Fig. 8: Same examples as in Fig. 7: Blocking over the BS on 10 July 2002 (left) and blocking over the NA on 19 June 2001 (right) concerning different meteorological parameters: (a,d) SLI in K, (b,e) PW in kg m^{-2} and (c,f) OMEGA in hPa h^{-1} .

Fig. 9: Anomaly composites during blocking over the BS (left) and over the NA (right) for (a,d) SLI in K, (b,e) PW in kg m^{-2} and (c,f) OMEGA in hPa h^{-1} with respect to the reference period (1981 – 2010). Black dots indicate statistically significant values.

Fig. 10: Same as Fig. 9, but for DLS in m s^{-1} .

Table 1. Annual number per year (left) and annual mean per month including standard deviation (right) of blocking events in the two areas NA and BS (cf. Fig. 5) during the investigation period.

Year	NA	BS	Month	NA	BS
2001	26	22	May	7.7 ± 2.5	4.9 ± 3.7
2002	17	38	June	7.1 ± 5.0	6.6 ± 4.6
2003	31	27	July	5.4 ± 3.1	9.5 ± 5.7
2004	26	16	August	6.4 ± 5.2	5.5 ± 2.9
2005	44	29			
2006	47	32			
2007	24	25			
2008	25	22			
2009	26	27			
2010	36	38			
2011	18	31			
2012	16	26			
2013	11	24			
2014	26	14			

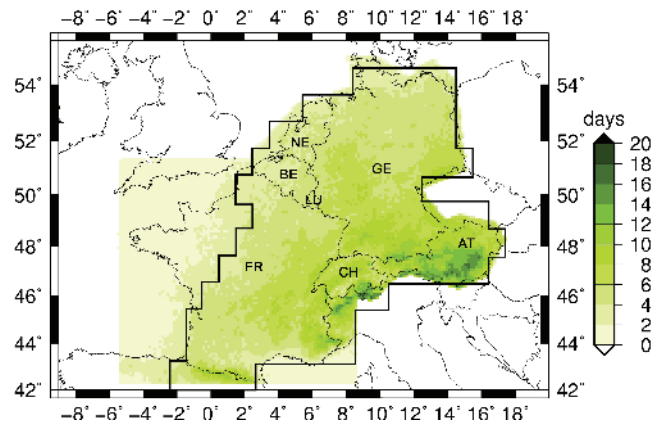


Figure 1 Mean annual number of thunderstorm days during May to August between 2001 and 2014 (FR = France, BE = Belgium, NE = Netherlands, LU = Luxembourg, GE = Germany, CH = Switzerland, AT = Austria.); the black line indicates the contiguous area of the 132 GPs referred to as FOCREG (see Chap. 3).

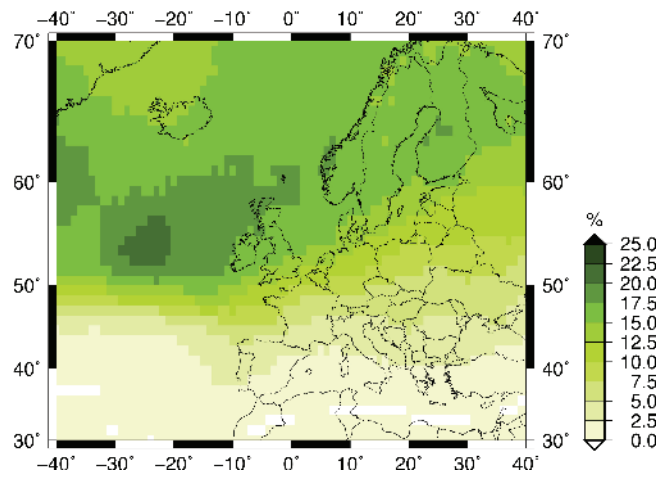


Figure 2. Relative blocking frequency between 2001 and 2014 (May – August).

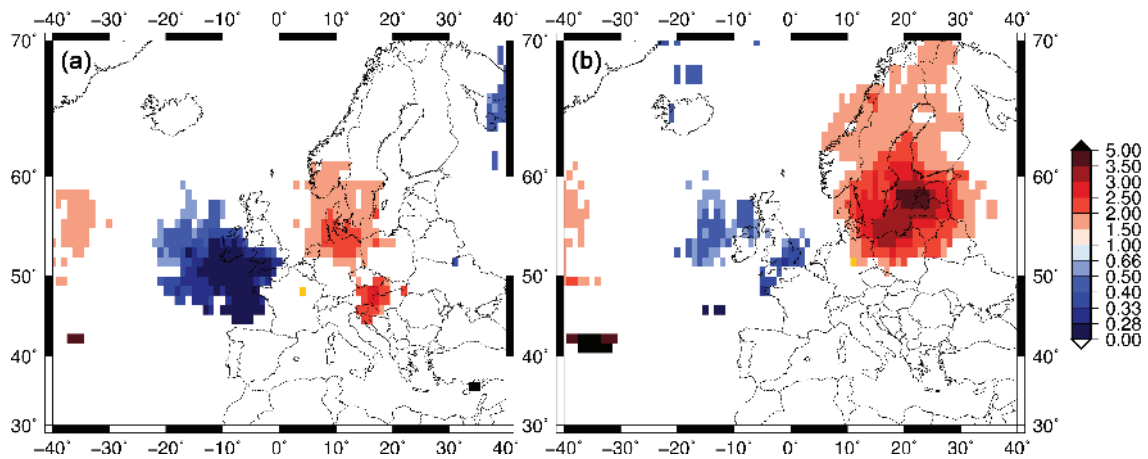


Figure 4. Two examples of identified areas with statistically significant (p-value at 95% significance level) changes in the odds ratio, where blocking affects the thunderstorm activity in two reference regions: (a) 48°N 4°E and (b) 52°N 11°E (illustrated as orange grid point). The blue colours indicate a reduction of thunderstorm days by blocking (e.g., a value of 0.5 means a decrease of the odds by 50%) and red colours indicate an increase (e.g., a value of 2 means a doubling of the odds).

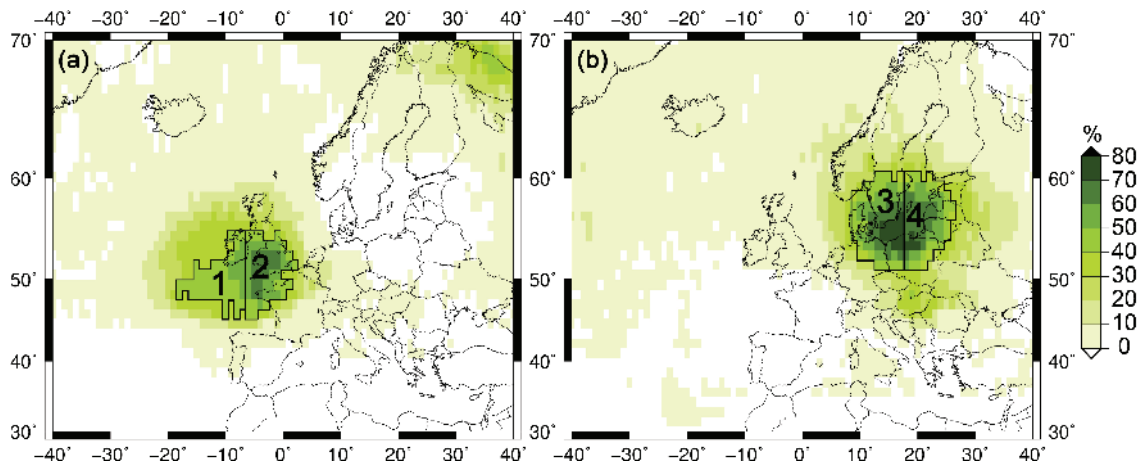


Figure 3. Relative frequency of the 132 OR calculations quantifying how often (a) $OR < 1$ (blocking suppresses TDs; blue in Fig. 3) or (b) $OR > 1$ (blocking supports TDs; red in Fig. 3). The black lines indicate the threshold₁ with 40%. The numbers define the sub-areas over the North Atlantic (1 = West and 2 = East) and the Baltic Sea (3 = West and 4 = East) for further investigations.

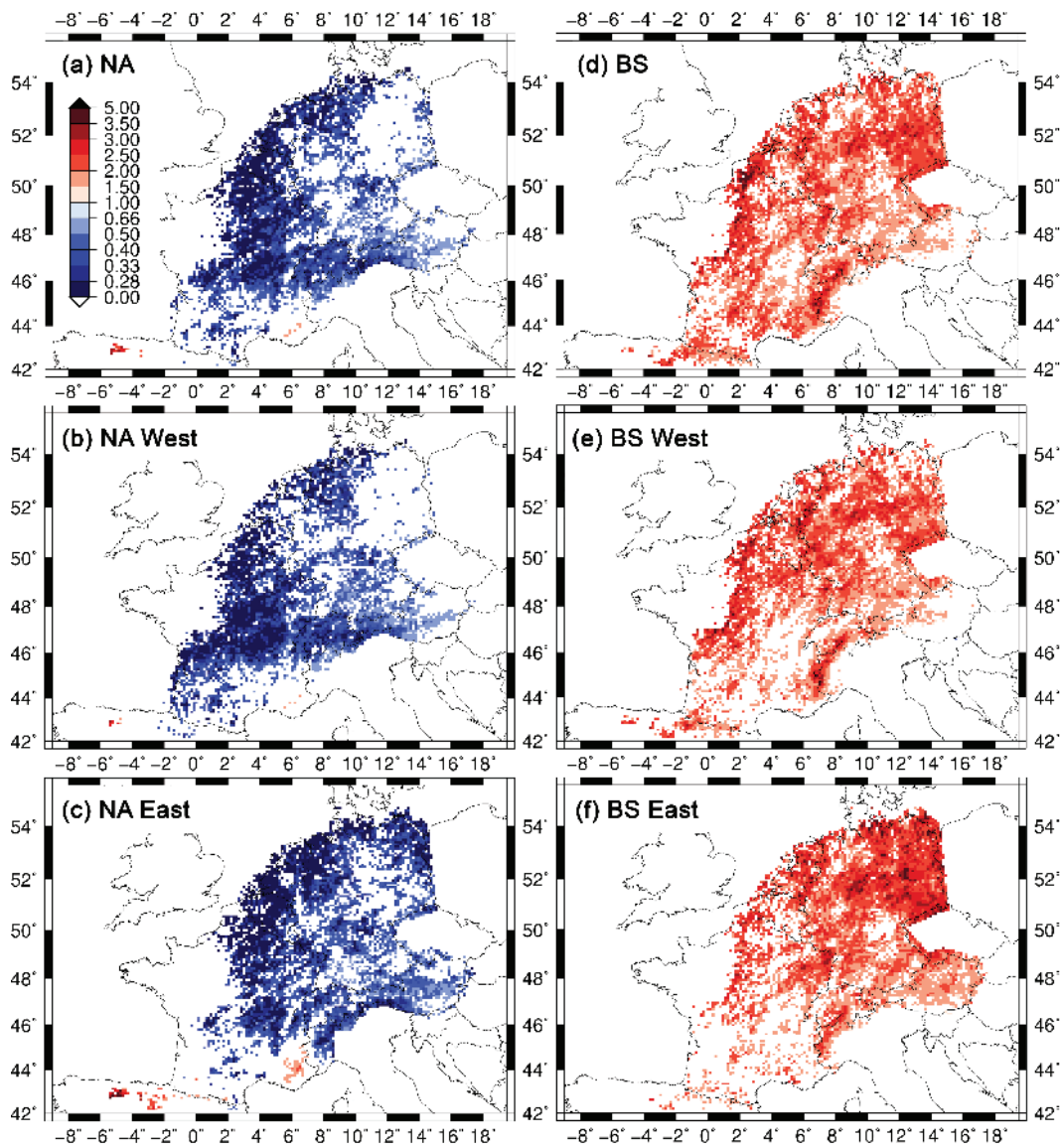


Figure 5. Same as Fig. 3; but for the six areas (defined in Fig. 4): (a-c) North Atlantic (NA) and (d-f) Baltic Sea (BS) with their respective sub-areas (b) NA West & (c) NA East and (e) BS West & (f) BS East. Note only values with a OR with p-value of at least 95% significance level are shown.

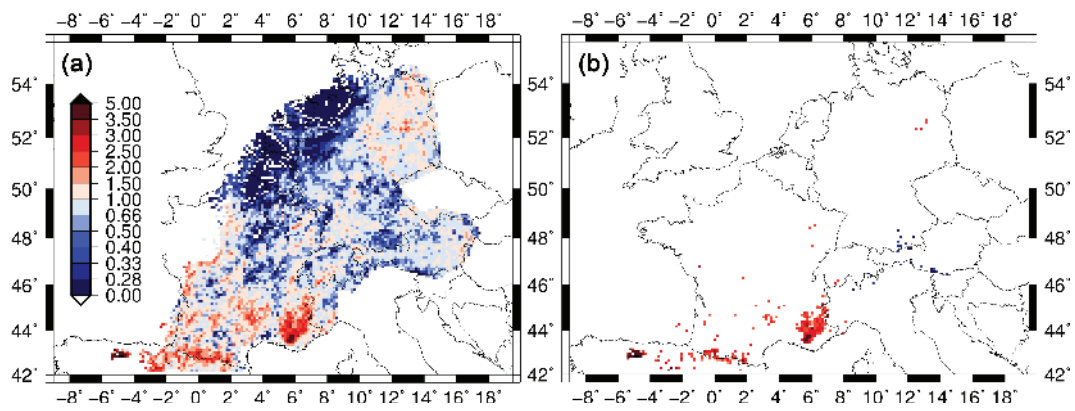


Figure 6 Same as Fig. 3; but for the crossover cases. Shown are (a) changes in the odds ratio at every grid point and (b) only grid points with statistically significant values at 95 % significance level).

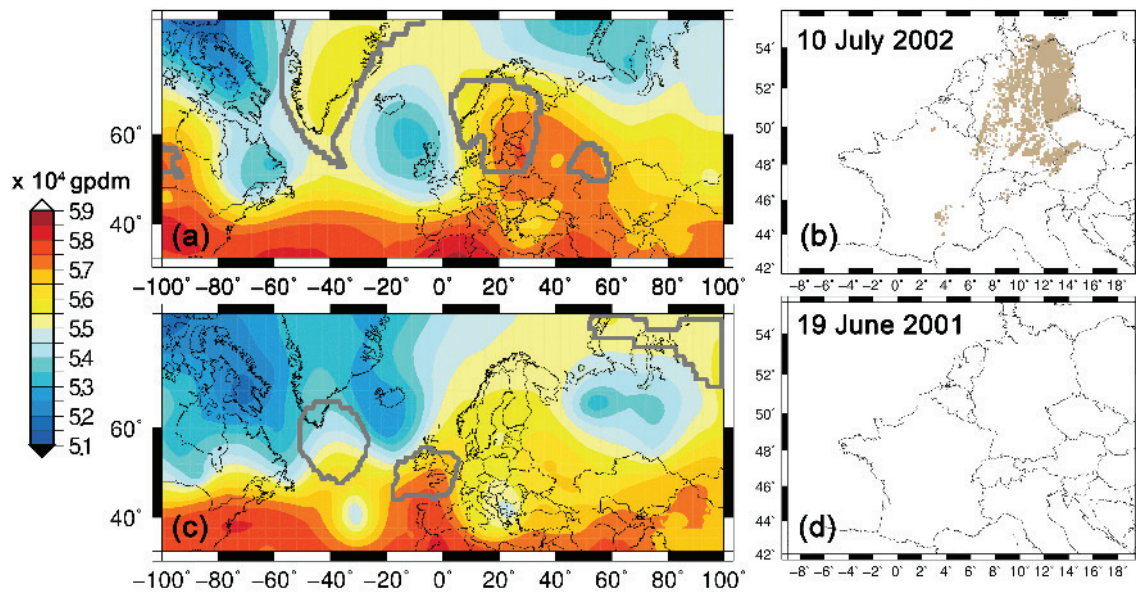


Figure 7. Examples of blocking events on 10 July 2002 over the NA (top) and on 19 June 2001 over the BS (bottom): (a,c) Φ_{500} in gpdm with blocks (grey contour) and (b,d) thunderstorm day (yes in beige).

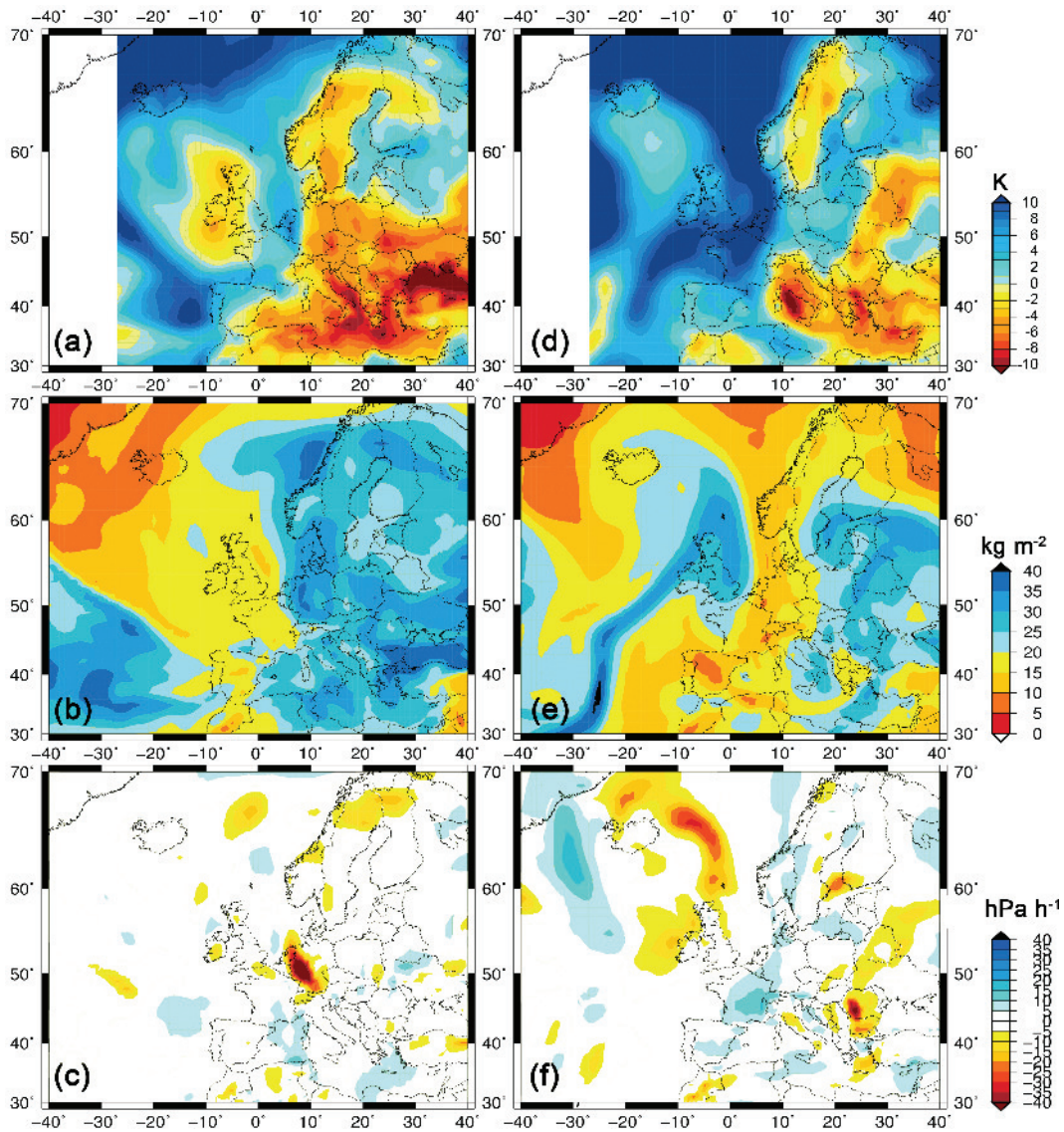


Figure 8. Same examples as in Fig. 7: Blocking over the BS on 10 July 2002 (left) and blocking over the NA on 19 June 2001 (right) concerning different meteorological parameters: (a,d) SLI in K, (b,e) PW in kg m^{-2} and (c,f) OMEGA in hPa h^{-1} .

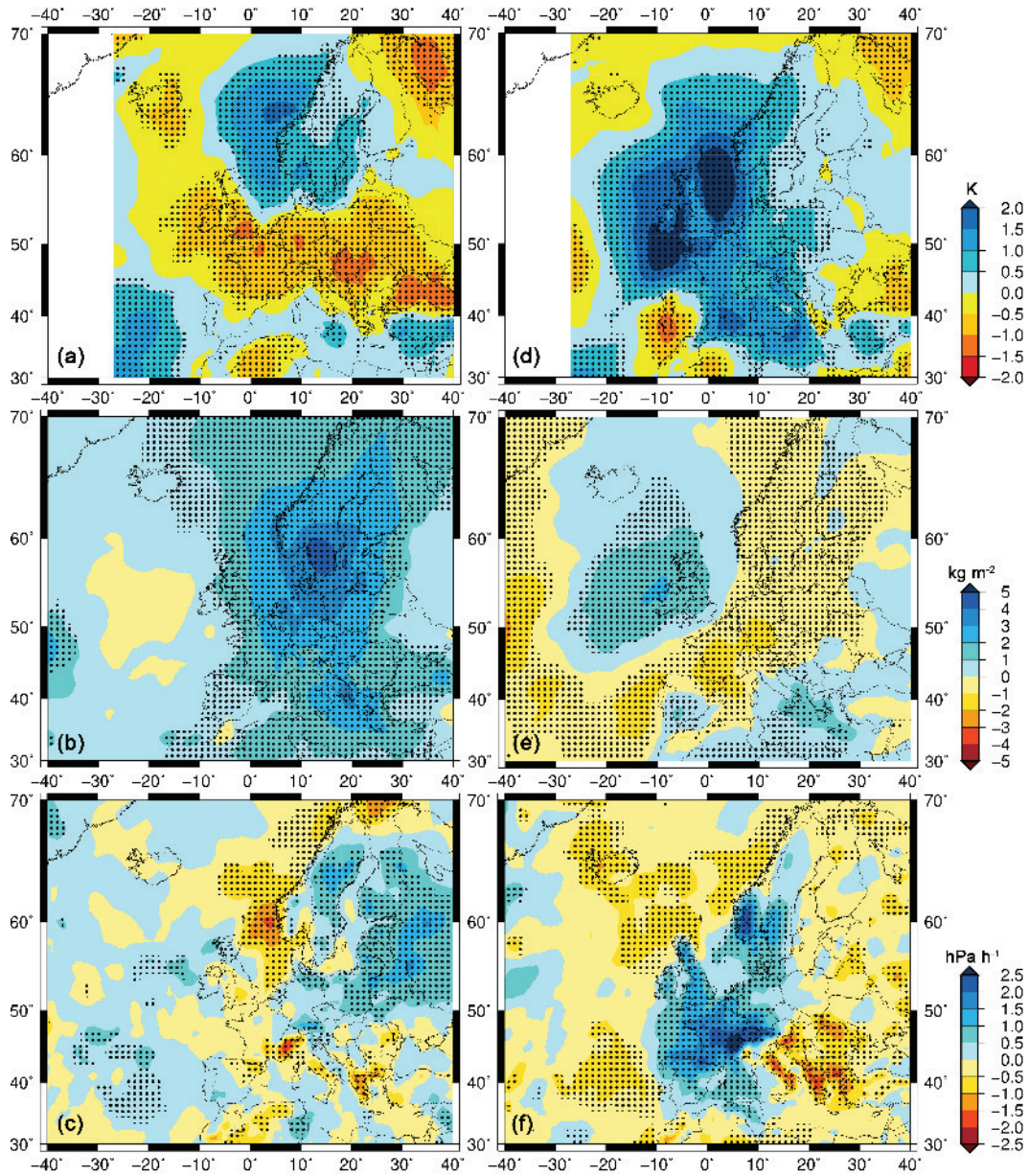


Figure 9. Anomaly composites during blocking over the BS (left) and over the NA (right) for (a,d) SLI in K, (b,e) PW in kg m^{-2} and (c,f) OMEGA in hPa h^{-1} with respect to the reference period (1981–2010). Black dots indicate statistically significant values.

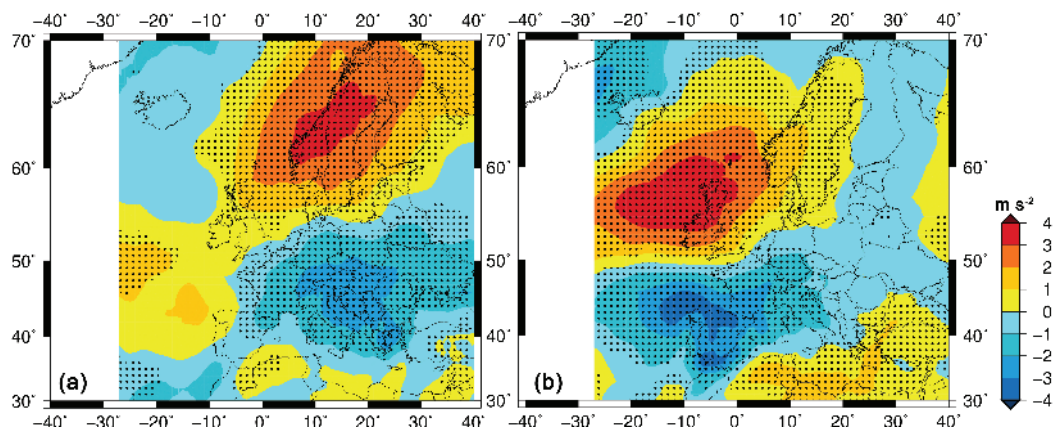


Figure 10. Same as Fig. 9, but for DLS in m s^{-1} .